Change of Macroscopic and Microscopic Symmetry of Barium Titanate Single Crystal around Curie Temperature

1998 Jpn. J. Appl. Phys. 37 5385

(http://iopscience.iop.org/1347-4065/37/9S/5385)

Jpn. J. Appl. Phys. Vol. 37 (1998) pp. 5385–5393
Part 1, No. 9B, September 1998

Change of Macroscopic and Microscopic Symmetry of Barium Titanate Single Crystal around Curie Temperature

Satoshi WADA, Takeyuki SUZUKI, Minoru OSADA[1], Masato KAKIHANA[1] and Tatsuo NOMA

Department of Applied Chemistry, Tokyo University of Agriculture & Technology, 24-16 Nakamachi 2-chome, Koganei, Tokyo 184-8588, Japan
[1]*Materials & Structures Laboratory, Tokyo Institute of Technology, 4259 Nagatsuta-cho, Midori-ku, Yokohama 226-8502, Japan*

(Received May 6, 1998; accepted for publication July 17, 1998)

Using a high-quality barium titanate single crystal grown by a top-seeded solution growth method, its microscopic and macroscopic symmetries were investigated by Raman scattering measurement and polarizing microscopy, respectively. Moreover, their temperature dependences through Curie temperature were also studied. As a result, we found that the microscopic symmetry of P4mm observed at room temperature did not change through Curie temperature. On the other hand, the macroscopic symmetry on the basis of a insitu domain observation was P4mm below 133°C and Pm3m above the Curie temperature. This difference between microscopic and macroscopic symmetries above the Curie temperature suggests that the barium titanate single crystal above the Curie temperature intrinsically exhibits some disorder behavior. On the basis of the results obtained in this study, the phase transition model of barium titanate single crystal with both displacive and order-disorder behaviors was proposed.

KEYWORDS: barium titanate, single crystal, microscopic symmetry, macroscopic symmetry, Curie temperature, Raman scattering, insitu domain observation

1. Introduction

Barium titanate $BaTiO_3$ is one of the "well-known" ferroelectrics with a Curie temperature of around 130°C. Its physical, electrical, optical, and elastic properties have been investigated by many researchers.[1–9] At present, it is believed that $BaTiO_3$ is one of the "well-analyzed" ferroelectric materials, and that there are few "unknown" areas about various properties of $BaTiO_3$. Recently, however, the development of new measurement equipment and preparation methods has led to new revelations of the various properties of $BaTiO_3$. One of the new results reported is the size and defect effects on $BaTiO_3$ fine crystal.[10,11]

Frey and Payne prepared fine $BaTiO_3$ nanocrystals whose diameter is below 100 nm using the sol-gel method, and reported the difference in symmetry obtained from XRD analysis and Raman scattering, i.e., the local symmetry from Raman scattering is assigned to an orthorhombic phase while the symmetry from XRD analysis assigned to a cubic phase.[10] Wada *et al.*, who prepared fine $BaTiO_3$ nanocrystals with an average diameter of 67 nm by a hydrothermal method, found that as-prepared hydrothermal $BaTiO_3$ nanocrystals contain hydroxyl groups in their lattices.[11] As a result of symmetry measurement of hydrothermal $BaTiO_3$ nanocrystals with a high concentration of lattice hydroxyl groups, the local symmetry from Raman scattering and infrared reflection measurement was assigned to a tetragonal phase (P4mm) while the symmetry from XRD analysis was assigned to a cubic phase (Pm3m). Moreover, it should be noted that from XRD analysis, the cell volume of Pm3m became larger than that of P4mm, and from Raman scattering measurement, the frequency and intensity of the observed phonon modes did not change despite the change in XRD while only the damping factor changed with the change in XRD. These behaviors look like the typical order-disorder behavior.

In general, XRD measurement uses the very static diffraction phenomenon of X-ray on several atomic planes of a crystal. Thus, XRD can be used to determine an average symmetry and a static one in a large region (coherence length over 2–3 nm) over a longer time (over 1 ms).[12] On the other hand, the physical phenomenon measured by Raman scattering and IR reflection spectroscopy is lattice vibration, i.e., a phonon that can occur in a coherence length below 2–3 nm within a very short time of less than 1 ns. Thus, the phonon is a very dynamic phenomenon. Raman scattering and IR spectroscopy can show a local and dynamic symmetry in a much smaller region (coherence length below 2–3 nm) within a much shorter time (below 1 ns).[13]

The kind of measured symmetry is dependent on the measured physical phenomenon with a coherence length (=spatial magnitude) and a time scale. Therefore, it is very important to clarify the kinds of methods used for symmetry measurement. Table I shows the relationship between the measurement method and the spatial magnitude and time scale of a measured physical phenomenon. It can be easily expected that by using the different measurement methods, even if the same material is used, different symmetries with various spatial magnitudes and time scales can be observed, because of the observation of different physical phenomena. In other words, it is very important to investigate several symmetries with different spatial magnitudes and time scales us-

Table I. The relationship between the measurement method and the spatial magnitude and time scale of a measured physical phenomenon.

Spatial magnitude d \ **Time scale** t	Microscopic $t < 1$ ns	Mesoscopic 1 ns$<t<$10 μs	Macroscopic 10 μs$<t$
Microscopic $d<$1–2 nm	Raman scattering spectroscopy		
Mesoscopic 2 nm$<d<$0.5 μm			X-ray diffraction analysis
Macroscopic 0.5 μm$<d$			Polarizing microscopy

ing the same material by different methods. We believe that several symmetry measurements are necessary to study about the phase transition of ferroelectrics.

Therefore, as regards the size effect on $BaTiO_3$ nanocrystals and the defect effect on $BaTiO_3$ nanocrystals with a high concentration of lattice hydroxyl groups, the difference in symmetries obtained from XRD analysis and Raman scattering suggests that there are some disordered behaviors in the crystal structure of $BaTiO_3$ nanocrystal. We propose that the size effect on ferroelectrics should be the phase transition from the ferroelectric phase to the paraelectric phase caused by crystalline size reduction. Thus, this concept can lead to the following prediction that the ideal $BaTiO_3$ single crystal should intrinsically have the disordered behavior in the phase transition at the Curie temperature. To confirm this prediction, several symmetry measurements must be done through the Curie temperature.

Through this manuscript, we describe the three kinds of symmetries as follows: we call the local and dynamic symmetry assigned by Raman scattering measurement (a) ***microscopic symmetry***, the average and static symmetry assigned by XRD analysis (b) ***mesoscopic symmetry***, and the macro and static symmetry assigned by domain observation using a polarizing microscope (c) ***macroscopic symmetry***. The spatial magnitude and the time scale for each symmetry are listed in Table I.

In this study, we used $BaTiO_3$ single crystals grown by the top-seeded solution growth method which now was recognized as the $BaTiO_3$ single crystal with the highest chemical and physical quality. We also measured its microscopic and macroscopic symmetries by Raman scattering and polarizing microscopy. Moreover, the temperature dependence of the microscopic and macroscopic symmetries, specially below and above the Curie temperature of around 130°C, was measured, and the difference between the microscopic and macroscopic symmetries observed above the Curie temperature was discussed. Finally, we proposed a schematic phase transition model on the basis of the results obtained in this study.

2. Experimental

2.1 Sample

The $BaTiO_3$ single crystals used here were prepared by a top-seeded solution growth (TSSG) method at Fujikura Ltd. The crystals had very high purity, and the concentration of most impurities (Cr, Mn, Fe, Co, Ni, Cu) was below 2–3 ppm.[14,15] The Ba/Ti atomic ratio was determined to be 1.000 by inductively coupled plasma (ICP) spectroscopy.[14] Chemical analysis revealed that this $BaTiO_3$ single crystal had excellent chemical quality, and there were very few lattice defects due to impurities. Optically, the crystal was transparent and lightyellow. The details of preparation of $BaTiO_3$ single crystals and their characterization are described elsewhere.[14,15] These crystals were oriented along [001] using a back-reflection Laue method, cut and polished to mirrorfinish. All characterizations and treatments were done at Fujikura Ltd.

2.2 Observation of microscopic symmetry

Microscopic symmetry was measured by Raman scattering spectroscopy. As the sample, a single-domain $BaTiO_3$ single crystal ($a : 3.63 \times b : 4.03 \times c : 4.16\,mm^3$; here, a, b, and c are parallel to a-axis, b-axis and c-axis, respectively.) was used. The single-domain treatment was done at Fujikura Ltd., and its details are described elsewhere.[14,16,17] Raman scattering was performed using a Raman scattering spectrometer with a triple monochromator (Jobin-Yvon, T64000). The $BaTiO_3$ single crystal (the top and bottom planes are (001) planes.) was placed in a cryostat with a high-purity quartz window, and was outgassed under vacuum for 20 hours prior to measurement. The final vacuum pressure in the cryostat was around 10^{-6} Torr.

The (100) plane of the $BaTiO_3$ single crystal was excited by a 50 mW Ar ion laser. The incident laser light polarized along [001] with a wavelength of 514.5 nm was focused to an almost 3-μm-diameter spot on the (100) plane using an optical microscope with a 90× long-working-distance lens. The power of the laser light incident on the surface of the crystal was maintained below $20\,W/cm^2$ in order to minimize possible thermal damage. The scattered light in the backward scattering geometry was passed through an analyzer polarized along [001] or [010], analyzed using a triple-grating spectrometer, and collected with a liquid nitrogen cooled CCD detector for 30 s. The slits were set to give a spectral resolution of around $3\,cm^{-1}$. The Raman spectra for $A_1(TO)$ and $B_1(TO)$ modes were measured from $50\,cm^{-1}$ to $900\,cm^{-1}$ in the $X(ZZ)\bar{X}$ geometry while E(TO) modes were measured from $100\,cm^{-1}$ to $900\,cm^{-1}$ in the $X(ZY)\bar{X}$ geometry.

Temperature just below the bottom of the crystal was measured, and was changed from 21.7°C to 200°C using a step function, i.e., temperature was increased at a rate of 0.5°C/min and after keeping the temperature constant for 20 min at various temperatures, Raman spectra were measured. The temperature in the cryostat was measured with an accuracy of ±1 °C and controlled within ±0.1 °C.

2.3 Observation of macroscopic symmetry

Macroscopic symmetry was measured using a polarizing microscope. As the sample, a multidomain $BaTiO_3$ single crystal oriented along [001] was used. The $BaTiO_3$ single crystal was polished to a final thickness of around 50 μm. Moreover, both top and bottom (001) surfaces of the crystal were mirror-finished. This extremely thin crystal was prepared for observation of detailed domain configuration. Since the domain configuration depends on the crystal's macroscopic symmetry, it is very important to interpret the domain configuration for the determination of macroscopic symmetry. The domain configuration was observed under crossed nicols in a transmittance geometry using a polarizing microscope (Carl Zeiss, D-7082).

The thin crystal was placed into a cryostat with an optical-isotropic glass window in air. Temperature just below the bottom of the crystal was measured, and then changed from 30°C to 200°C using a step function, i.e., temperature was increased at a rate of 5°C/min and after keeping the temperature constant at various temperatures for 10 min, the domain configuration was observed. The temperature in the cryostat was measured with an accuracy of ±1 °C and controlled within ±0.5 °C.

3. Results and Discussion

3.1 Temperature dependence of microscopic symmetry

3.1.1 A_1 and B_1 modes in $BaTiO_3$ single crystal

Raman scattering measurement was done in two kinds of backward scattering geometries, i.e., X(ZZ)$\bar{X}$ and X(ZY)$\bar{X}$ geometries (X, Y and Z mean *a*-axis, *b*-axis and *c*-axis, respectively). Throughout this manuscript, the scattering configuration is denoted by A(BC)$\bar{A}$, which means that the incident light polarized along the B direction propagates along the A direction, and the scattered light polarized along the C direction propagates along the opposite A direction (i.e., $\bar{A}$). The polar direction of tetragonal $BaTiO_3$ single crystal at room temperature is the [001] direction. Therefore, Raman scattering measurement in X(ZZ)$\bar{X}$ geometry results in the Raman scattering spectra of the A_1 and B_1 transverse optic (TO) modes, while Raman scattering measurement in X(ZY)$\bar{X}$ geometry results in the Raman scattering spectra of the E transverse optic (TO) mode.

Moreover, in the Raman scattering measurement using the backward scattering geometry, we must consider the presence of a distorted surface layer of $BaTiO_3$ single crystal, which might be induced by polishing. To confirm the effect of this surface layer, some Raman spectra were measured at room temperature using the backward scattering geometry, the forward scattering geometry and the 90° scattering geometry. As a result, almost the same Raman spectra were obtained using the three kinds of the scattering geometries. Thus, it could be confirmed that the effect of the surface layer on the Raman scattering spectra is negligible, and in this study, the backward scattering geometry was used.

The Raman scattering spectrum of A_1 and B_1 modes at room temperature is shown at the bottom of Fig. 1. Resonance frequencies of A_1(1TO), A_1(2TO), B_1(1TO) and A_1(3TO) modes were observed around 180, 280, 308, and 515 cm^{-1}, respectively. These modes completely corresponded to the A_1(TO) and B_1(TO) modes of tetragonal $BaTiO_3$ single crystal reported by Scalabrin *et al.*;[18] thus, it is clear that the microscopic symmetry of our $BaTiO_3$ single crystal can be assigned to P4mm. Moreover, in the Raman scattering spectrum of A_1 and B_1 modes at room temperature, there is no longitudinal optic (LO) mode; thus, it was confirmed that the laser beam cross section is in a truly single-domain state.

In this spectrum, it should be noted that only the A_1(3TO) mode shows an asymmetric shape. In general, lattice vibration can be expressed as the harmonic damped oscillator, and each phonon mode must be a symmetric shape. Therefore, the asymmetrically shaped peak should be considered as the overlapping of two symmetrically shaped peaks, i.e., the "true" A_1(3TO) mode and an "unknown" mode. Kall reported that in high-T_c superconductors, the asymmetric shape is usually due to the interaction of "normal" phonon with crystal defects and other phonons.[19] Moreover, he also reported that similar to other phonons, the phonon mode deviated slightly from the "normal" phonon mode for some reason. The magnitude of deviation from the "normal" phonon is a maximum in the phonon mode that includes the lightest ion. In $BaTiO_3$ single crystal, the A_1(3TO) mode is the O_6 octahedra deformation mode along [001] direction, and it is expected that in $BaTiO_3$, if there is a phonon mode that deviates most from the "normal" phonon mode; this mode must be the A_1(3TO) mode that includes only the lightest ion, i.e., oxygen. In this study, it was suggested that there exists an "unknown" mode in TSSG-grown $BaTiO_3$ single crystal at room temperature.

To date, many researchers have reported the measurement of Raman scattering spectra using $BaTiO_3$ single crystals prepared by various methods, and all A_1(3TO) modes in their spectra have an asymmetric shape.[18,20–26] In this study, although we used the TSSG-grown $BaTiO_3$ single crystal that had less impurity than those and "excellent" chemical quality, the A_1(3TO) mode in the spectra was also asymmetric. If this "unknown" mode originated from lattice defects such as "symmetry breaking defect", it would be expected that the degree of asymmetry at the A_1(3TO) mode in our crystal becomes smaller than those in other previous reports. However, there is little difference among all A_1(3TO) modes. Therefore, it is possible that $BaTiO_3$ can intrinsically have some fluctuation behavior that deviates from the "normal" phonon mode. At present, however, it is very difficult to assign this "unknown" mode to either a mode induced by the lattice defect or a deviated intrinsic mode from "normal" phonon.

The temperature dependence of A_1 and B_1 modes was measured from 21.7°C to 200°C, and the results are shown in Figs. 1 and 2. With increasing temperature from 21.7°C to 140°C, the resonance frequency of each mode decreased slightly while the damping factor (=FWHM of peak) of each mode broadened. The patterns of these spectra, however, did not change significantly, which suggests that the microscopic symmetry of $BaTiO_3$ single crystal is still assigned to P4mm

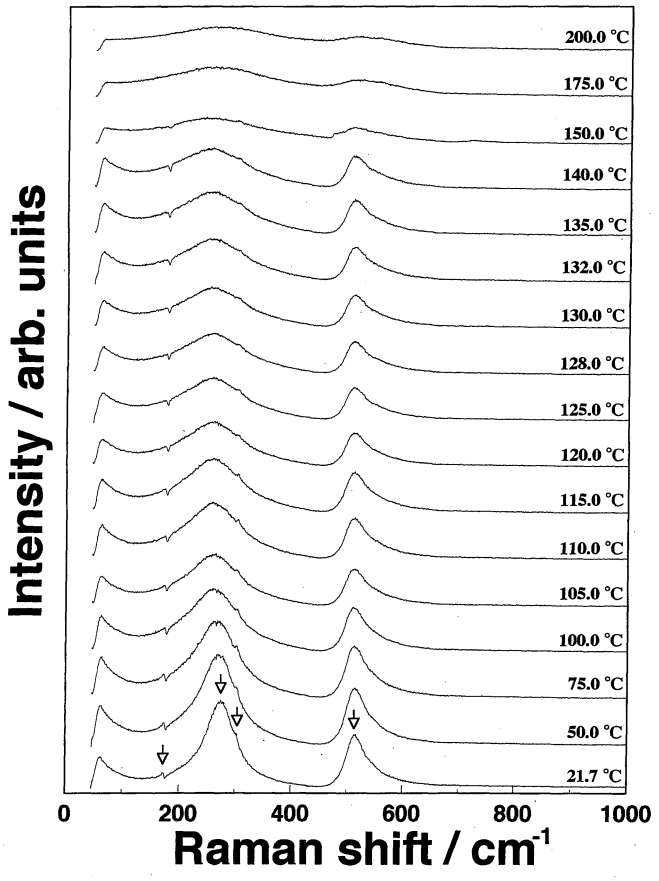

Fig. 1. Temperature dependence of A_1(TO) and B_1(TO) modes in $BaTiO_3$ single crystal.

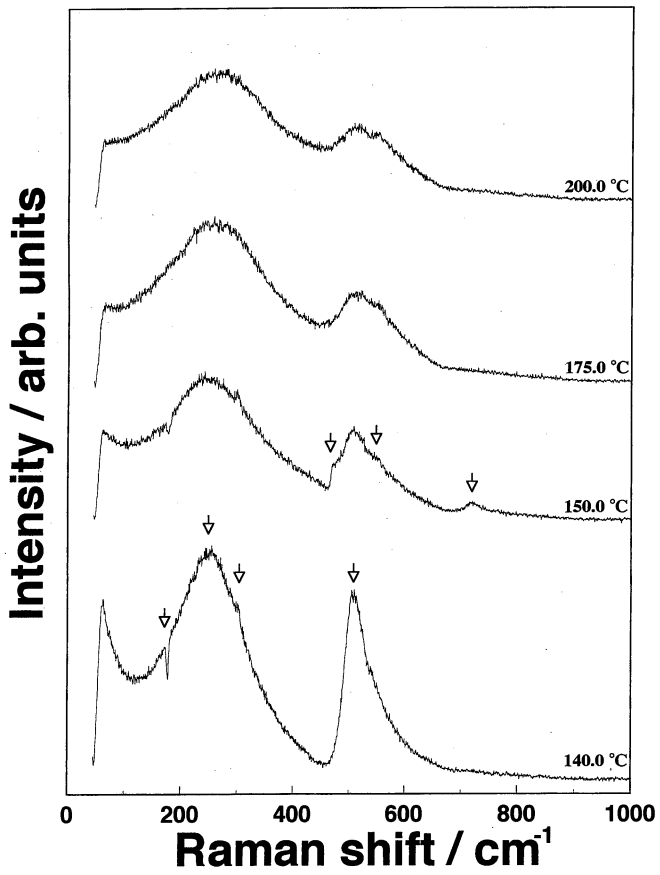

Fig. 2. Temperature dependence of A_1(TO) and B_1(TO) modes in $BaTiO_3$ single crystal (magnified view).

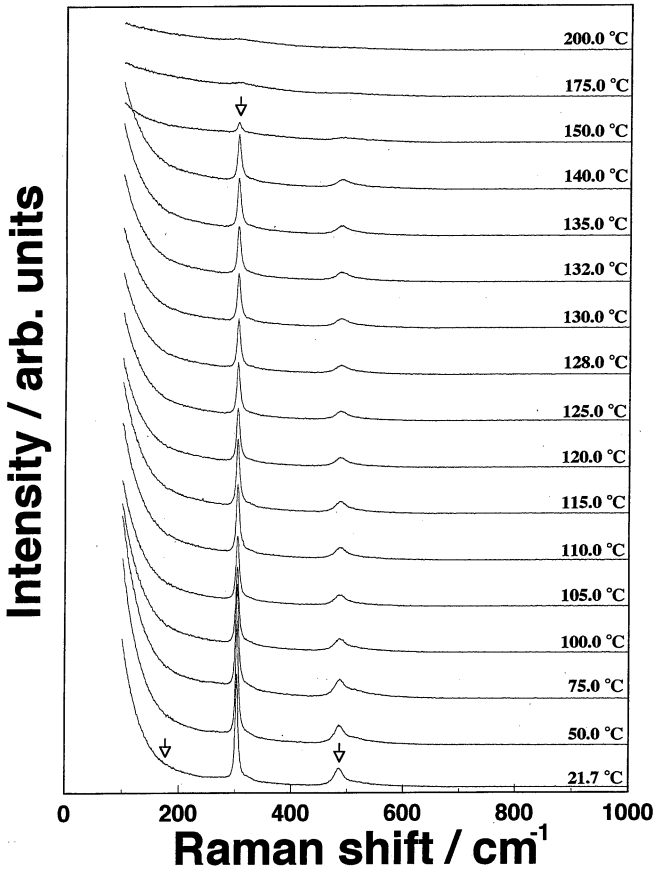

Fig. 3. Temperature dependence of E(TO) modes in $BaTiO_3$ single crystal.

at 140°C.

On the other hand, at 150°C (Fig. 2), two new peaks suddenly appeared, i.e., a small peak around 470 cm^{-1} and a broad peak around 720 cm^{-1}. These two peaks were assigned to the A_1(2LO) mode around 470 cm^{-1} and the A_1(3LO) mode around 720 cm^{-1}, and these assignments agreed completely with that reported by Scalabrin *et al.*[18] The appearance of LO modes means that at 150°C, there can exist a region (i.e., ferroelectric domain) whose polar direction is parallel to the incident and scattering light in $BaTiO_3$ single crystal. This indicates that at 150°C, the single-domain state changed to multidomain one.

Moreover, the separation of the A_1(3TO) mode with an "unknown" mode was observed clearly in Fig. 2. This supports the validity of the assumption that the asymmetrically shaped A_1(3TO) mode should be due to the overlapping of two symmetrically shaped peaks. Moreover, the Raman intensity of the "normal" A_1(3TO) mode decreased at 150°C while that of the "unknown" mode showed little change. Therefore, it seems that the origin of the "unknown" mode is not related to that of the other modes.

As regards the other modes, except for the A_1(2LO) and the A_1(3LO) modes, their Raman intensities at 150°C were less than half of those at 140°C, and their FWHM was over 1.5 times of those at 140°C. However, their resonance frequency did not change. Therefore, this revealed that although the damping factor increased and thus the lifetime of the phonon became much shorter, the microscopic symmetry of the $BaTiO_3$ single crystal at 150°C was still P4mm. This P4mm microscopic symmetry was observed even at 200°C.

3.1.2 E modes of $BaTiO_3$ single crystal

The temperature dependence of the E modes of $BaTiO_3$ single crystal was measured from 100 cm^{-1} to 900 cm^{-1} in the $X(ZY)\bar{X}$ geometry. We also measured the E mode from 3.53 cm^{-1} to 700 cm^{-1} in order to study the soft mode (i.e., Slater mode); however, the results are described elsewhere.[27] The Raman scattering spectrum of E modes at room temperature is shown in the bottom of Fig. 3. The resonance frequencies of E(2TO), E(3TO) and E(4TO) modes, except for the E(1TO) mode (i.e., the soft mode), were observed around 180 (very weak), 310, and 490 cm^{-1}, respectively. All these modes completely corresponded to the E(TO) modes of tetragonal $BaTiO_3$ single crystal reported by Scalabrin *et al.*[18] Therefore, these results support the result obtained from that in A_1 and B_1 modes, which the microscopic symmetry of the $BaTiO_3$ single crystal can be assigned to P4mm. Moreover, in the Raman scattering spectrum of E modes at room temperature, no LO mode exists; thus, it was confirmed that the laser beam cross section is truly a single-domain state.

In the E(4TO) mode, an asymmetric shape similar to that of the A_1(3TO) mode was observed. We can also separate the asymmetric E(4TO) mode into the "normal" E(4TO) mode and an "unknown" mode. The E(4TO) mode is also the O_6 octahedra deformation mode along [100] and [010] directions, and the origin of its vibration mode is the same as that of the A_1(3TO) mode. As has been described in the previous section, it is expected that the "unknown" mode can be assigned to the mode that induces the lattice defects or the phonon mode that deviates from the "normal" E(4TO) mode.

Figures 3 and 4 show the temperature dependence of the E(TO) modes measured from 21.7°C to 200°C. With increasing temperature from 21.7°C to 140°C, the resonance frequency of each mode did not change while the FWHM of each mode broadened. The patterns of these spectra also did not change, which suggests that the microscopic symmetry of $BaTiO_3$ single crystal is still assigned to P4mm at 140°C.

On the other hand, at 150°C (Fig. 4), no new peak appeared in the E modes, in contrast with the result of the A_1 modes. Thus, the transformation from the single-domain state to a multidomain one at 150°C cannot be confirmed from the result of the E modes. At present, we cannot explain this difference between A_1 and E modes. However, the separation of the "normal" E(4TO) mode from the "unknown" mode was observed despite their large linebroadening in Fig. 4. This fact supports the validity of the assumption that the asymmetrically shaped E(4TO) mode consists of two overlapping symmetric peaks. Moreover, at 150°C, the Raman intensity of the "normal" E(4TO) mode decreased while that of the "unknown" mode showed little change. Therefore, it seems that the origin of the "unknown" mode is unrelated to that of the other modes. This phenomenon observed in E modes agrees completely with that in A_1 modes.

At 150°C, the Raman intensity of E(3TO) and E(4TO) modes decreased suddenly, while their FWHM increased remarkably. However, their resonance frequency did not change as shown in Fig. 4. This indicates that although the damping factor increased and the lifetime of the phonon became much shorter, the microscopic symmetry of $BaTiO_3$ single crystal at 150°C was P4mm. This P4mm microscopic symmetry was observed even at 200°C. This phenomenon observed in E modes also agrees completely with that in A_1 modes.

However, one question remains about the reliability of the temperature values measured during Raman scattering, because our Raman scattering spectra changed significantly at 150°C, although many researchers reported that the Curie temperature of $BaTiO_3$ is around 130°C.[1-9,14-18,20-26] We measured the temperature using a thermocouple positioned immediately below the bottom of the crystal while Raman scattering measurement was conducted in a small region 2 μm from the top surface and about 4mm from the thermocouple. Moreover, the crystal was placed on the heater in a high vacuum of around 10^{-6} Torr, and heat conduction from the bottom to the top depended on only the phonons. Therefore, this crystal height of 4mm may be the origin of the temperature difference between the top and the bottom of the crystal. As described in the next section, the insitu domain observation showed that when the multidomain state of $BaTiO_3$ single crystal changed to the optical isotropic state gradually and partially at 133°C, many new domains were created and disappeared during this phase transition. The temperature measured during the insitu domain observation has higher precision, because crystal was only 50 μm thick, and the crystal was placed on the heater in air. Therefore, it is reasonable that the temperature of 150°C measured in Raman scattering corresponds to 133°C. This is because in Raman scattering measurement, the change from the single-domain state to a multidomain one, i.e., the creation of new domains, was observed at 150°C. On the basis of the results of domain observation, the correction of temperature measured in Raman scattering is shown in Table II.

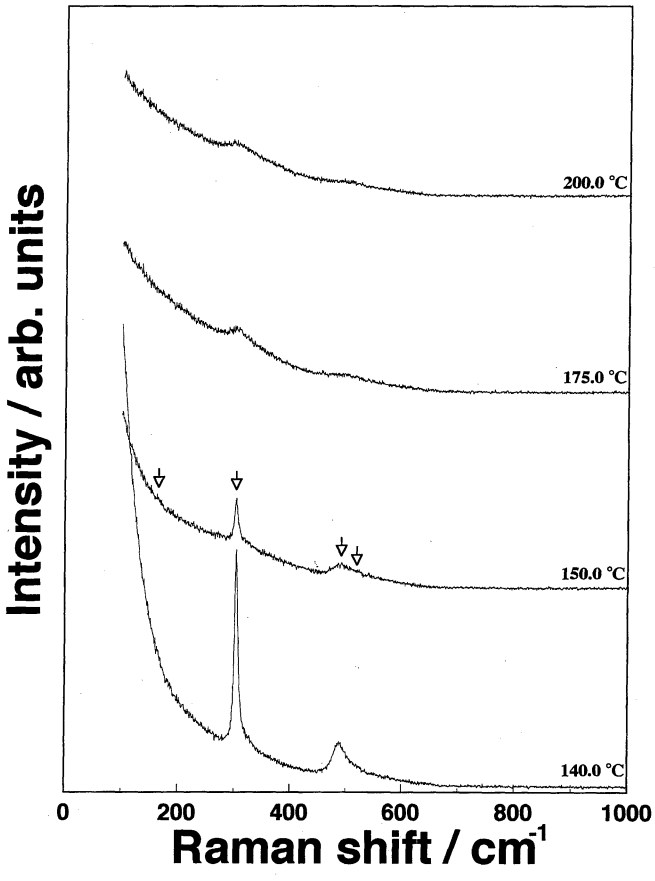

Fig. 4. Temperature dependence of E(TO) modes in $BaTiO_3$ single crystal (magnified view).

3.2 *Temperature dependence of macroscopic symmetry*

Insitu domain observation was always done under crossed

Table II. Temperatures (I) during Raman scattering measurements and temperatures (II) that were corrected based on the results of insitu domain observation.

Temperature I (°C)	Temperature II (°C)
21.7	21.7
50.0	46.2
75.0	67.9
100.0	89.6
105.0	93.9
110.0	98.3
115.0	102.6
120.0	106.9
125.0	111.3
128.0	113.9
130.0	115.6
132.0	117.3
135.0	119.9
140.0	124.3
150.0	133.0
175.0	154.6
200.0	176.3

nicols in the transmittance configuration. The extremely thin multidomain $BaTiO_3$ single crystal oriented along [001] was placed directly on the heater in air, and its temperature was measured using a thermocouple positioned immediately below the crystal. Therefore, the use of the measured temperature as the sample temperature should have high accuracy because of very small crystal thickness around 50 μm and the transmittance configuration.

Figure 5 shows the typical domain configuration of a multidomain $BaTiO_3$ single crystal at room temperature. Under a fixed angle of the polarizer and the analyzer, when only the crystal was rotated, the extinction position in the total crystal region was observed at 90° despite its multidomain state. This indicated that the polar direction of all domains does not lie along [001] direction of the crystal, but lies along [100] and [010] directions (i.e., normal to the polarized light). Therefore, this configuration is a 90° domain configuration, and its macroscopic symmetry is assigned to the tetragonal phase (P4mm).[28]

The temperature dependence of its domain configuration was observed from 30.3°C to 200°C. Figure 6 shows the typical domain configurations at various temperatures. All domain configurations were observed in the diagonal position determined from Fig. 6(a). In the domain configurations at 30.3°C and 130°C (Figs. 6(a) and 6(b)), no change was evident, and the macroscopic symmetry in each domain was assigned to P4mm at 130°C.

On the other hand, at 133°C, initially the optical isotropic region appeared partially, accompanied by the formation of many new fine domains, and the coexistence of the optical isotropic phase and the ferroelectric phase was observed, as shown in Fig. 6(c). This formation of many new domains originated from the coexistence of the two phases. This is because the lattice volume of the optical isotropic phase is smaller than that of the ferroelectric P4mm phase, and interfacial stress is expected to occur at the interface between the two phases. Therefore, we think that this stress is the origin of the formation of the new domains.

The area of the optical isotropic phase increased with time, and finally most of the crystal changed to the optical isotropic phase (Fig. 6(d)). Therefore, the shape of the indicatrix in this optical isotropic phase can be a perfect sphere, and its macroscopic symmetry is assigned to the highest cubic symmetry Pm3m.[28] This optical isotropic phase did not change from 133°C to 200°C as shown in Fig. 6(e).

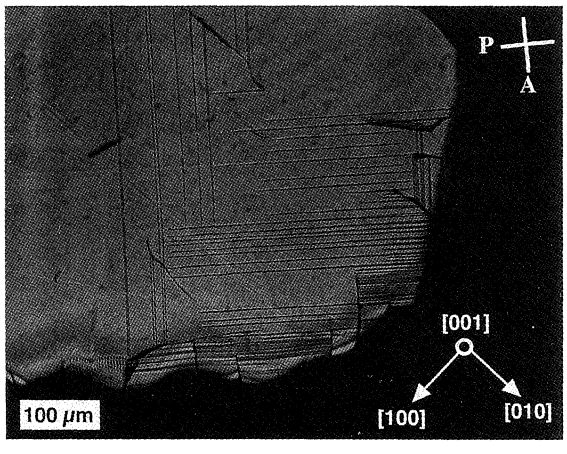

Fig. 5. Domain configuration of $BaTiO_3$ single crystal at 25°C.

To conclude, we confirmed that the macroscopic symmetry of $BaTiO_3$ single crystal was P4mm below 133°C while it was Pm3m above 133°C. The change in macroscopic symmetry observed in this study shows good agreement with the change in mesoscopic symmetry of $BaTiO_3$ single crystal observed using XRD which was reported by Kay and Vousden.[4]

3.3 *Crystal structure with disorder behavior of $BaTiO_3$ single crystal above Curie temperature*

Kurosaka *et al.* reported that DSC measurement of TSSG-grown $BaTiO_3$ single crystal resulted in the observation of the Curie temperature around 132°C.[14] In this study, the in-situ domain observation using a polarizing microscope also revealed the disappearance of domains and the appearance of the optical isotropic phase at 133°C, i.e., the change in macroscopic symmetry from P4mm to Pm3m at 133°C. Therefore, it is confirmed that phase transition in the macroscopic symmetry occurs at 133°C. However, Raman scattering measurement showed that although the Raman intensity decreased significantly and the damping factor increased at 133°C, the Raman spectra assigned to P4mm still remained at temperatures above 133°C. This means that at 133°C, the microscopic symmetry of P4mm did not change while the phonon state changed significantly.

The lack of change in microscopic symmetry at the Curie temperature of 133°C suggests that the phase transition at 133°C cannot be considered as a simple first-order displacive-type phase transition that was recognized by many researchers.[1–5] Since the microscopic symmetry of P4mm does not change below and above the Curie temperature, there must exist a very small polar region with a polar vector above the Curie temperature. However, because the macroscopic symmetry is the paraelectric phase of Pm3m above the Curie temperature, the polar direction of the small polar region must be flipping among six equivalent directions of ⟨001⟩ within a very short time. In order to understand this phenomenon, we must consider the "super-paraelectric model" to explain the relaxor behavior proposed by Cross.[29] However, it should be noted that the flipping frequency in $BaTiO_3$ at temperatures above 133°C may be higher as much as by 10^3–10^6 than that in the relaxor.

In this study, it should be noted that the microscopic symmetry of P4mm did not change through 133°C while the phonon state changed significantly at 133°C. In particular, the damping factor of the observed phonon modes increased suddenly at the Curie temperature. The increase in damping factor means the shortening of the phonon lifetime, i.e., the shortening of the phonon propagation length, in the damped oscillator. On the other hand, all resonance frequencies of the phonon modes did not change through the Curie temperature, i.e., there is no change in vibration energy of the phonon modes. Why is it that only the damping factor changed abruptly at the Curie temperature?

It is well known that the coupling of only one specific phonon mode with free electrons, photons, and other factors with energy state almost similar to the phonon energy state results in the increase in only its FWHM and the formation of an asymmetric shape.[13,19,30] However, in this study, the increase in damping factor of all phonon modes was observed.

This suggests that at 133°C, a factor that can affect the vibration state of all the observed phonons appeared suddenly. What is this factor? One possible factor is the flipping behavior of a polar vector in the polar region. Assuming that the polar vector in the polar region can flip among six equivalent ⟨001⟩ directions within some time that is almost of the same order as the lattice vibration time and that this flipping time has some distribution, we can explain the phenomenon observed in this study. At present, we have no proof to support this assumption.

This assumption, however, can be supported by the experimental results reported by Burns and Dacol.[31] In the refractive index measurement of $BaTiO_3$ single crystal above the Curie temperature, they found that a phase with spontaneous polarization $\boldsymbol{P}$ was formed at 300°C, because at temperatures between the Curie temperature and 300°C, no optical property proportional to $\boldsymbol{P}$ was observed while the property proportional to $\boldsymbol{P}^2$ could be detected. This result suggested the "flipping" behavior of the polar vector, and supported the order-disorder behavior. Moreover, Takahashi proposed a theoretical model for the phonon in the $BaTiO_3$ crystal. Above the Curie temperature, there is a strong local order (polar phase with a fixed polar direction) in the ferroelectric disordered phase (unpolar phase with flipping polar direction), and the phase transition at the Curie temperature is a complete order-disorder transition.[32]

However, we cannot agree completely with his model although we can accept a part of his model. This is because we cannot completely deny the displacive-type behavior. The results obtained in this study suggest the presence of the order-disorder behavior in the microscopic symmetry at the Curie temperature, but do not deny the contribution of the displacive-type behavior to the phase transition at the Curie temperature. Moreover, the statistic pressure dependence of the phase transition behavior of $BaTiO_3$ single crystal, which was reported by Samara, supported strongly the claim that the phase transition at the Curie temperature must be the first-order displace-type phase transition.[33] Therefore, at present we think that the phase transition at 133°C is the displace-

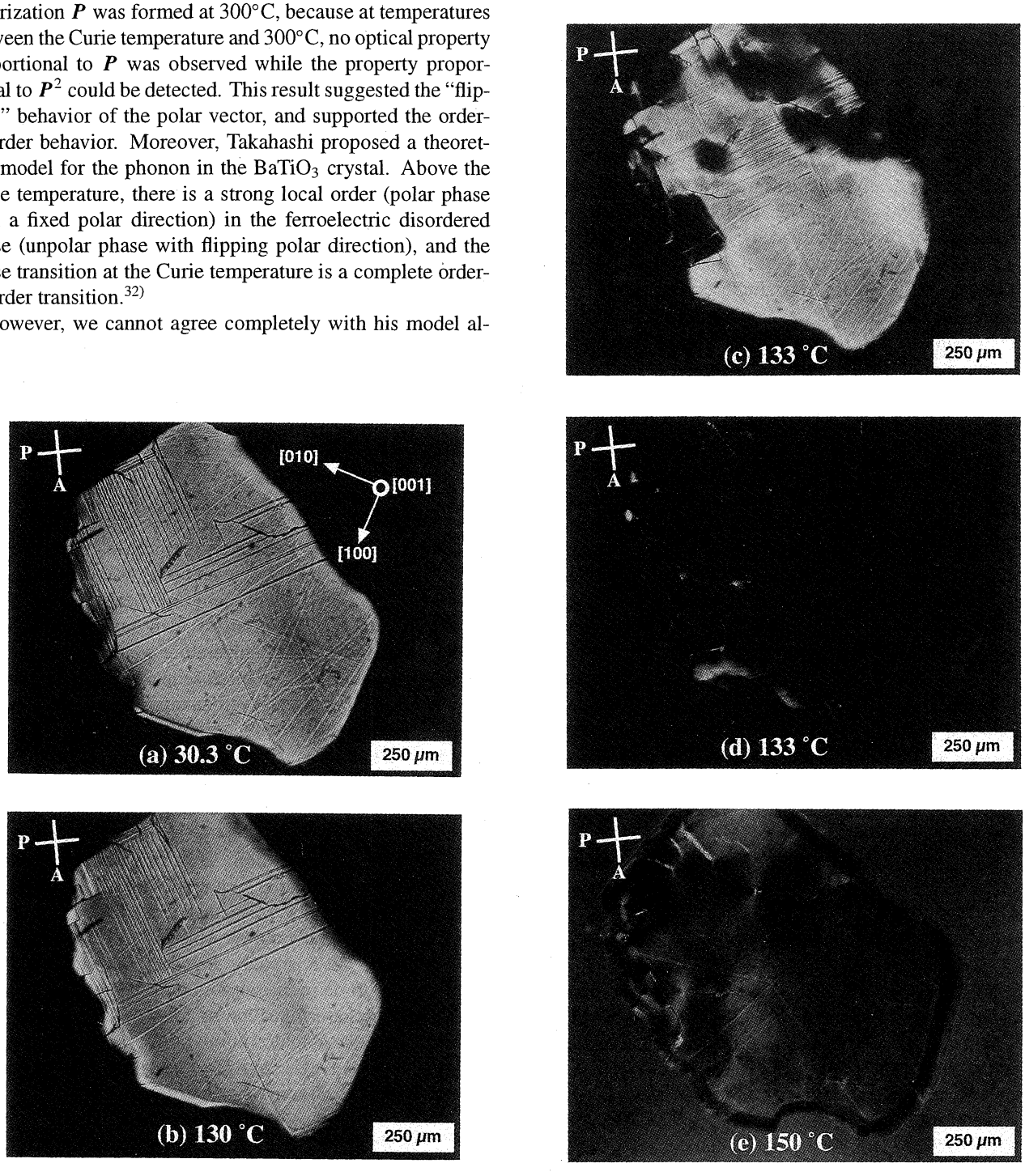

Fig. 6. Temperature dependence of domain configuration of $BaTiO_3$ single crystal.

type phase transition accompanied by the order-disorder type behavior.

Some models were proposed to explain the disorder behavior. First, we must consider the "CLG" model proposed by Comes *et al.*[34] in order to explain the results of diffuse X-ray scattering measurements on all the phases of $BaTiO_3$ and $KNbO_3$ crystals.[34,35] In particular, in the cubic phase of $BaTiO_3$ single crystal above the Curie temperature, the CLG model proposes that for Ti ions in a cubic lattice, their most stable position is the position shifted from the center to the body diagonal ⟨111⟩ directions. Moreover, all Ti ions in the one-dimensional region with a length of 10–20 lattices can be displaced along the same one direction among eight equivalent ⟨111⟩ directions while all Ti ions in the neighboring one-dimensional region can also be displaced along another ⟨111⟩ direction different from neighboring chain. They called this the "chain structure". Therefore, since each lattice loses its center of symmetry, above the Curie temperature, the cubic phase can have Raman active phonons. However, the average symmetry in the region with many chain structures can be assigned to cubic phase from XRD analysis.

In the Raman scattering measurement of $BaTiO_3$ single crystals in the 1960's, the presence of some peaks above the Curie temperature was observed by many investigators, but they could not assign them precisely because of the limitation of equipment and $BaTiO_3$ single crystal samples.[20–26] Therefore, the CLG model was considered to be one of the reasonable models for the Raman peaks observed above the Curie temperature. In this study, however, we revealed that all Raman peaks observed above the Curie temperature were assigned to P4mm using the TSSG-grown $BaTiO_3$ single crystal with the highest quality and excellent equipment with the triple monochromator. This means that Ti ions must be displaced along the ⟨001⟩ directions above the Curie temperature. Therefore, the CLG model is not a reasonable model for the origin of Raman peaks above the Curie temperature although it is a fact that the X-ray scattering measurement using cubic $BaTiO_3$ single crystal above the Curie temperature showed strong anisotropy in the diffuse scattering patterns. Previously, we proposed the "phase transition model with both displacive and order-disorder behaviors", in order to explain the phenomenon observed in the "size" effect on the symmetry of hydrothermal $BaTiO_3$ fine particles.[11,36] Here, we try to explain the disorder behavior and the diffuse scattering behavior above the Curie temperature using the following new modified phase transition model with both displacive and order-disorder behaviors.

In $BaTiO_3$ single crystal, when temperature was decreased from high temperature over 300°C, the microscopic symmetry changed from Pm3m to P4mm around 300°C. This phase transition around 300°C is a displacive-type structural phase transition due to the displacement of ions. However, the magnitude of the polar vector $\boldsymbol{P}$ in the unstable and small polar region (i.e., polar micro region (PMR)) around 300°C is very small and its polar direction flips among six equivalent directions along ⟨001⟩. Here, the concept of PMR is as follows: PMR is completely different from a domain with a fixed polar vector, and its region as well as polar directions can change with time. This is because the barrier energy ΔG for the polarization around 300°C is much lower than the thermal energy kT. Since this flipping time is very short, the mesoscopic and macroscopic symmetries measured by XRD and a polarizing microscope must be assigned to Pm3m. Direct observations of PMR have never been reported to date, but some reports were made on quasi-elastic scattering with strong anisotropy in neutron, X-ray and electron scattering measurements above 133°C. These phenomena suggests indirectly the existence of PMR in $BaTiO_3$ single crystal above the Curie temperature.

Moreover, with decreasing temperature from 300°C to 133°C, the magnitudes of polar vector $\boldsymbol{P}$ and ΔG for the polarization increased while kT decreased, and then the energy difference between ΔG and kT became small. Finally, when temperature reaches 133°C, all flipping behaviors of the polar vector freeze simultaneously. There is the coexistence of order-disorder and displacive type phase transitions. Owing to the frozen polar directions, the mesoscopic and macroscopic symmetries measured using XRD and a polarizing microscope can be assigned to P4mm, and thus the drastic phase transition is observed. On the other hand, the microscopic symmetry measured using Raman and IR remains as P4mm and does not change through Curie temperature.

The above model is only schematic. To refine and modify the model, much investigative work must be done at temperatures immediately above the Curie temperature. We will conduct other measurements for this purpose. Now, we have a great question about the simple concept classifying the phase transition of ferroelectrics into the displacive and order-disorder type, or the first-order and second-order type. This is because most ferroelectric material such as $BaTiO_3$ single crystal seem to exhibit both behaviors during their phase transition at the Curie temperature. In the future, we will have to develop a new concept to express the phase transition behavior.

4. Conclusions

Using high-quality $BaTiO_3$ single crystals grown by the TSSG method, its microscopic and macroscopic symmetries were investigated by Raman scattering measurement and polarizing microscopy. Moreover, their temperature dependences through the Curie temperature were also studied. As a result, we found that the microscopic symmetry P4mm of $BaTiO_3$ single crystal observed at room temperature did not change with increasing temperature through the Curie temperature and that the microscopic symmetry above the Curie temperature was P4mm. On the other hand, the macroscopic symmetry on the basis of insitu domain observation of $BaTiO_3$ single crystal was P4mm below 133°C and Pm3m above the Curie temperature. This difference between microscopic and macroscopic symmetries above the Curie temperature suggests that the structure of $BaTiO_3$ single crystal above the Curie temperature intrinsically exhibits some disorder behavior. In this study, however, we were unable to obtain results to deny the contribution of the displacive behaviors to the phase transition at 133°C. Therefore, on the basis of the results obtained in this study, the phase transition model of $BaTiO_3$ single crystal with both the displacive and order-disorder behaviors was proposed.

Acknowledgements

We would like to thank Dr. A. Kurosaka and Mr. O. Nakao of Fujikura Ltd. for preparing the TSSG-grown $BaTiO_3$ single

crystals with excellent chemical quality. We also would like to thank Dr. L. E. Cross, Dr. T. R. Shrout and Dr. S.-E. Park of MRL, Pennsylvania State University for their helpful discussions about the analysis of the domain configuration, and Dr. H. Ikawa of Kanagawa Institute of Technology for helpful discussions about the phase transition of barium titanate.

1) B. Matthias and A. von Hippel: Phys. Rev. **73** (1948) 1378.
2) W. P. Mason: Phys. Rev. **74** (1948) 1134.
3) W. J. Merz: Phys. Rev. **91** (1953) 513.
4) H. F. Kay and P. Vousden: Philos. Mag. **40** (1949) 1019.
5) M. E. Caspari and W. J. Merz: Phys. Rev. **80** (1950) 1082.
6) A. Schaefer, H. Schmitt and A. Dorr: Ferroelectrics **69** (1986) 253.
7) O. Nakao, K. Tomomatsu, S. Ajimura, A. Kurosaka and H. Tominaga: Appl. Phys. Lett. **61** (1992) 253.
8) T. Ishidate and S. Sasaki: J. Phys. Soc. Jpn. **56** (1987) 4212.
9) M. Zgonik, P. Bernasconi, M. Duelli, R. Schlesser, P. Gunter, M. H. Garrett, D. Rytz, Y. Zhu and X. Wu: Phys. Rev. **50** (1994) 5941.
10) M. H. Frey and D. A. Payne: Phys. Rev. B **54** (1996) 3158.
11) T. Noma, S. Wada, M. Yano and T. Suzuki: J. Appl. Phys. **80** (1996) 5223.
12) B. D. Cullity: *Elements of X-ray Diffraction* (Addison-Wesley, Reading, 1978) 2nd ed., p. 82.
13) K. Kudo: *Optical Properties of Materials* (Ohmu Press, Tokyo, 1990) 2nd ed., p. 298 [in Japanese].
14) A. Kurosaka, K. Tomomatu, O. Nakao, S. Ajimura, H. Tominaga and H. Osanai: J. Soc. Mater. Eng. Res. **5** (1992) 74 [in Japanese].
15) S. Ajimura, K. Tomomatu, O. Nakao, A. Kurosaka, H. Tominaga and O. Fukuda: J. Opt. Soc. Am. B: **9** (1992) 1609.
16) O. Nakao, K. Tomomatsu, S. Ajimura, A. Kurosaka and H. Tominaga: Jpn. J. Appl. Phys. **31** (1992) 3117.
17) O. Nakao, K. Tomomatsu, S. Ajimura, A. Kurosaka and H. Tominaga: Ferroelectrics **156** (1994) 135.
18) A. Scalabrin, A. S. Chaves, D. S. Shin and S. P. S. Porto: Phys. Status Solidi B **79** (1977) 731.
19) M. Kall: Dr. Thesis, Chalmers University of Technology, Chalmers, 1995.
20) J. L. Parson and L. Rimai: Solid State Comm. **5** (1967) 423.
21) M. DiDomenico, S. H. Wemple, S. P. S. Porto and R. P. Bauman: Phys. Rev. **174** (1968) 522.
22) M. P. Fontana and M. Lambert: Solid State Commun. **10** (1972) 1.
23) A. M. Quittet and M. Lambert: Solid State Commun. **12** (1973) 1053.
24) G. Burns and F. H. Dacol: Phys. Rev. B. **18** (1978) 5750.
25) B. Jannot, L. Gnininvi and G. Godefroy: Ferroelectrics **37** (1981) 669.
26) J. A. Sanjurjo and R. S. Katiyar: Ferroelectrics **37** (1981) 693.
27) S. Wada, T. Suzuki, T. Noma, M. Osada and M. Kakihana: submitted to J. Phys. Soc. Jpn.
28) E. E. Wahlstrom: *Optical Crystallography* (John Willey and Sons, New York, 1979) 5th ed., p. 208.
29) L. E. Cross: Ferroelectrics **76** (1987) 241.
30) G. Burns: *Solid State Physics* (Academic Press, Tokyo, 1985) Vol. 4, p. 118 [in Japanese].
31) G. Burns and F. H. Dacol: Ferroelectrics **37** (1981) 661.
32) H. Takahashi: J. Phys. Soc. Jpn. **16** (1961) 1685.
33) G. A. Samara: Proc. 2nd IMF 1969, J. Phys. Soc. Jpn. **28** (1970) p. 399.
34) R. Comes, M. Lambert and A. Guinier: Solid State Commun. **6** (1968) 715.
35) J. Harada and G. Honjo: J. Phys. Soc. Jpn. **22** (1967) 45.
36) S. Wada, T. Suzuki and T. Noma: J. Ceram. Soc. Jpn. **104** (1996) 383.